

## 5. Transmutation Research

Transmutation – the idea of changing one element into another – is almost as old as time itself. In the middle-Ages, the alchemists tried to turn base metals into gold. Transmutation, however, only became a reality in the last century with the advent of nuclear reactors and particle accelerators.

One of the main interests today in transmutation is in the field of nuclear waste disposal. Nuclear waste is a radioactive by-product formed during normal reactor operation through the interaction of neutrons with the fuel and container materials. Some of these radioactive by-products are very long-lived (long half-lives) and if untreated, must be isolated from the biosphere for very long times in underground repositories. Various concepts are being investigated worldwide on how to separate out (partition) these long-lived by-products from the waste and convert (transmute) them into shorter-lived products thereby reducing the times during which the waste must be isolated from the biosphere.

In the following sections, a brief history of attempts made to modify the decay constant, and thereby enhance the transmutation rate, is outlined. A particularly interesting application of transmutation is in the synthesis of super-heavy elements in which lighter elements are fused with heavier ones and transmuted to new elements. Finally, a new technique – laser transmutation – is described in which very high intensity laser radiation is used to produce high energy photons, and particles which can be used for transmutation studies.

### How Constant is the Decay Constant?

Following the discovery of radioactivity, many attempts to modify  $\alpha$  decay rates were made by changing temperature, pressure, magnetic fields, and gravitational fields (experiments in mines and on the top of mountains, using centrifuges). In one attempt, Rutherford [1] actually used a bomb to produce temperatures of 2500 °C and pressures of 1000 bar albeit for a short period of time. No effect on the decay constant was detected.

Only through Gamow theory of alpha decay could one understand why the above experiments to modify the decay constant were negative. Gamow showed that quantum-mechanical tunnelling through the Coulomb barrier was responsible for alpha emission. Even if the entire electron cloud surrounding a nucleus were removed, this would change the potential barrier by only a very small factor. Changes of the order of  $\delta k/k \approx 10^{-7}$  are to be expected.

In 1947, Segrè [2] suggested that the decay constant of atoms undergoing electron capture (ec) could be modified by using different chemical compounds of the substance. Different compounds will have different electron configurations and this should lead to small differences in the ec decay rate. This idea was confirmed experimentally using  $^7\text{Be}$ . This nuclide has a half-life of 53.3 d and decay by ec is accompanied by the emission of a 477.6 keV gamma photon. A comparison of  $\text{BeF}_2$  and Be revealed a difference in the decay rate  $\delta k/k = 7 \times 10^{-4}$ . These chemically induced changes in the decay constant are small but measurable.

It is also to be expected that the decay constant can be modified by pressure. As the pressure increases, the electron density near the nucleus should increase and manifest itself in an increase in the decay rate (for ec). Experiments [3, 4] on  $^{99\text{m}}\text{Tc}$ ,  $^7\text{Be}$ ,  $^{131}\text{Ba}$ , and  $^{90\text{m}}\text{Nb}$  have shown that this is indeed the case. The fractional change in the decay constant is  $\delta k/k \approx 10^{-8}$  per bar. At pressures of 100 kbar, which can be relatively easily produced in laboratory conditions,  $\delta k/k = 10^{-3}$  and the change in the decay constant is still small. Extrapolation to very high pressures would give  $\delta k/k \approx 10$  at 1 Gbar and  $\delta k/k \approx 10^3$  at 100 Gbar. With regard to  $\beta^-$  decay, it is also expected that screening effects can also modify the decay constant [5, 6].

Recently fissioning of  $^{238}\text{U}$  has been demonstrated using very high power laser radiation (see section on “Laser Transmutation”). The fact that through laser induced fission one can significantly alter the rate of fission is however not achieved through modifying the environment. It arises indirectly through bremsstrahlung and electron induced reactions with the nucleus. In the focal region, the beam diameter is 1  $\mu\text{m}$  and the penetration depth is 20 nm. In this region there are approximately  $10^9$  atoms of  $^{238}\text{U}$ . On average, every 10 y one of these atoms will decay by alpha emission. Spontaneous fission will occur on a timescale approximately six orders of magnitude longer, i.e.  $10^7$  y. Under irradiation by the laser, typically 8000 fissions are produced per pulse.

## Natural Transmutation by Radioactive Decay

Recently, ten years old  $^{244}\text{Cm}_2\text{O}_3$  particles of approximately 1 mm size have been analysed [7]. As the half-life of  $^{244}\text{Cm}$  is 18.1 years, approximately 55 to 60% of the initial curium had decayed into  $^{240}\text{Pu}$  producing an equal atomic fraction of helium (produced from the alpha particles). Now, even for a small inert atom such as helium, concentrations of this order of magnitude are hardly conceivable in the form of gas-in-solid; therefore, some form of bubble precipitation was expected to occur. Yet, the experiment showed that much more dramatic changes took place in the sample during ageing.

The microscopic observations of the sample, as well as the thermal annealing experiments on helium release reveal drastic restructuring phenomena. The initial granular structure has totally disappeared, and, though still geometrically compact, the sample consists of an intricate, spongy agglomeration of small globular particles of sizes of the order of a few microns.

Surprisingly, a number of morphologically diverse phases are formed during production of  $\alpha$ -damage. Some of them preserve traces of the original grains, others,

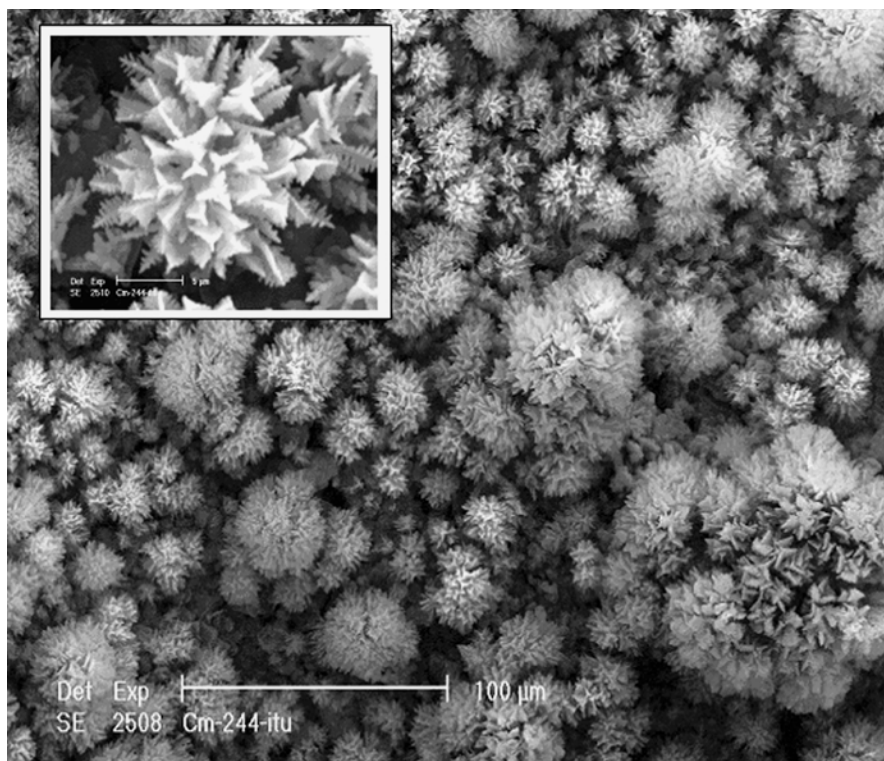


**Fig. 5.1.** Surface features of the curium oxide sample. Colonies of dendritic crystals are formed, likely due to re-deposition of recoil atoms. The inset shows a magnification of the dendrites [7]

formed on the sample outer surface, assumed coral-like configurations consisting of groups of regularly arranged platelets which often display a pronounced pine-tree dendrite shape (Fig. 5.1).

The “cauliflower” structure of Fig. 5.1, and the dendrites, can only originate from re-deposition of vaporised atoms produced by energetic recoils and sputtering events. This structure of the curium oxide sample is an example of natural transmutation on a macroscopic scale by radioactive decay.

## Synthesis of Superheavy Elements by Transmutation

The idea of the existence of a group of stable elements outwith the main nuclear “island” dates back to the 1930s and received considerable attention in the 1960s. The location of a smaller island of stability at  $Z = 114$ ,  $N = 184$  was suggested in 1966 and, at this time, prompted an intensive search for superheavy elements in nature. The isotope  $Z = 114$ ,  $N = 184$  has a doubly magic configuration with both the protons and neutrons being in complete shells. In addition, the idea of creating superheavy elements experimentally through heavy ion collisions led to a number

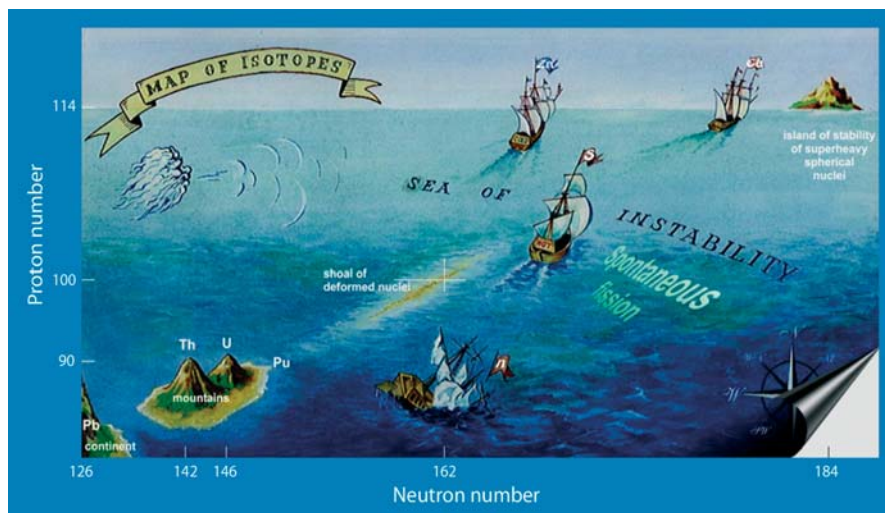
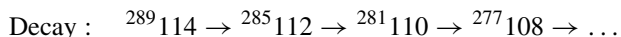
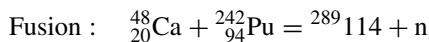


**Fig. 5.2.** The nuclide chart as depicted by Prof. Flerov in 1974. The ships, which are afloat, represent the different laboratory strategies and facilities dedicated to this endeavour (picture by Prof. G. N. Flerov, Dubna, USSR) [15]

of laboratories being set up to investigate this [8–10]. The wave of enthusiasm, at the time depicted in Professor Flerov’s Nuclide Chart shown in Fig. 5.2, continues to this day.

In the years 1981–84, the GSI group at Darmstadt, Germany, reported the synthesis of elements 107 (Bohrium), 108 (Hassium), and 109 (Meitnerium). In 1994 elements 110 (recently named Darmstadtium, Ds) and 111 (suggested name Roentgenium, Rg) were reported by the same group [11–13]. In 1998, a Russian team in Dubna claimed to have synthesized for the first time element 114 [14]. This was achieved by bombarding (fusing) nuclei of plutonium-242 with calcium-48. The scientists had to bombard the plutonium with calcium nuclei for a period of six weeks to produce a single nucleus of element 114. The reaction gives rise to a compound nucleus,  $^{289}_{114}$  shown below, which decays by alpha emission. The compound nucleus of element 114 had the remarkably “long” half-life of 30 s before undergoing a series of alpha decays to element 108 over a time period of approximately 30 minutes.



In 1999, researchers from the University of California at Berkeley and Oregon State University claimed to have detected three atoms of element 118 in collisions between high-energy krypton ions and a lead target. The results, however, were later retracted.

## Laser Transmutation

Recent advances in laser technology now make it possible to induce nuclear reactions with light beams [16–18]. When focussed to an area of a few tens of square microns,



**Fig. 5.3.** *Left:* Giant pulse VULCAN laser. Courtesy CCLRC Rutherford Appleton Laboratory. *Right:* High intensity Jena tabletop laser. Courtesy Institut für Optik und Quantenelektronik, Friedrich-Schiller-Universität, Jena

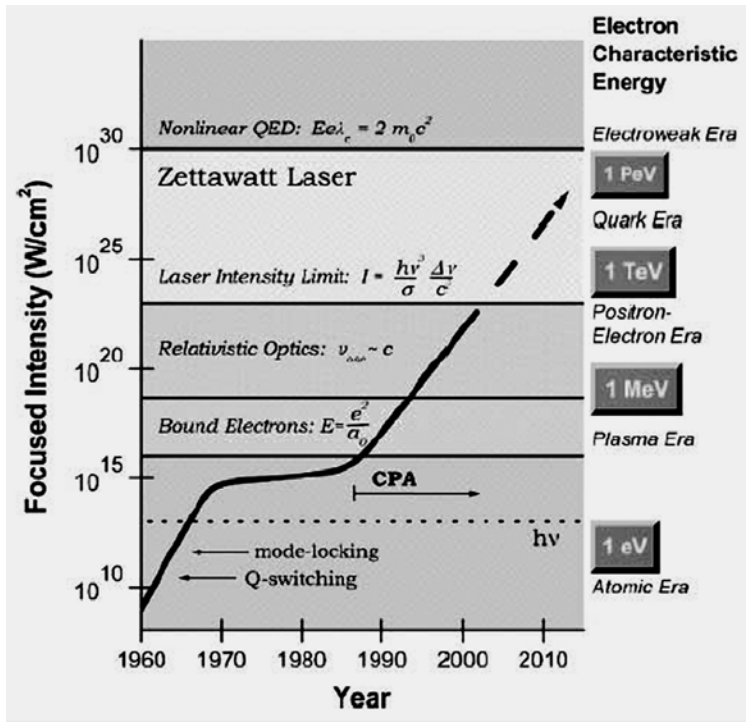


**Fig. 5.4.** Dramatic increase in focussed laser intensity over the past few decades for tabletop systems [19]. With the development of chirped pulse amplification (CPA) techniques in the mid-eighties, a new era of laser matter interactions has become possible

the laser radiation can reach intensities greater than  $10^{20} \text{ W cm}^{-2}$ . By focusing such a laser onto a target, the beam generates a plasma with temperatures of ten billion degrees ( $10^{10} \text{ K}$ ) – comparable to conditions that occurred one second after the ‘big bang’.

With the help of modern compact high intensity lasers, it is now possible to produce highly relativistic plasma in which nuclear reactions such as fusion, photo-nuclear reactions and fission of nuclei have been demonstrated to occur. Two decades ago, such reactions induced by a laser beam were believed to be impossible. This new development opens the path to a variety of highly interesting applications, the realisations of which require continued investigation of fundamental processes by both theory and experiment and in parallel the study of selected applications.

The possibility of accelerating electrons in focussed laser fields was first discussed by Feldman and Chiao [20] in 1971. The mechanism of the interaction of charged particles in intense electromagnetic fields, e.g. in the solar corona, had, however, been considered much earlier in astrophysics as the origin of cosmic rays. In this early work, it was shown that in a single pass across the diffraction limited focus of a laser power of  $10^{12}$  W, the electron could gain 30 MeV, and become relativistic within an optical cycle. With a very high transverse velocity, the magnetic field of the wave bends the particle trajectory through  $\mathbf{v} \times \mathbf{B}$  Lorentz force into the direction of the travelling wave. In very large fields, the particle velocity approaches the speed of light and the electron will tend to travel with the wave, gaining energy as it does so.

Dramatic improvements in laser technology since 1984 have revolutionised high power laser technology [21]. Application of chirped-pulse amplification techniques [22, 23] has resulted laser intensities in excess of  $10^{19}$  W cm<sup>-2</sup>. In 1985, C. K. Rhodes [23] discussed the possibility of laser intensities of  $\approx 10^{21}$  W cm<sup>-2</sup> using a pulse length of 0.1 ps and 1 J of energy. At this intensity, the electric field is  $10^{14}$  V cm<sup>-1</sup> a value which is over 100 times the coulomb field binding atomic

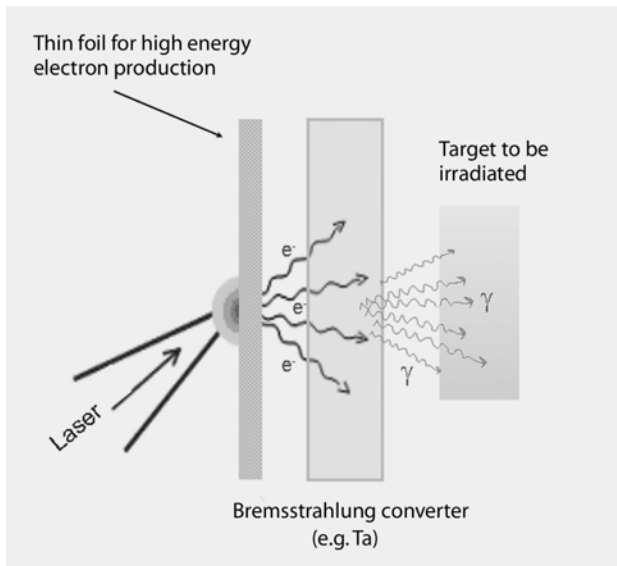


**Fig. 5.5.** Schematic setup of the laser experiments for high energy electron and photon generation

electrons. In this field, a uranium atom will lose 82 electrons in the short duration of the pulse. The resulting energy density of the pulse is comparable to a 10 keV blackbody (equivalent light pressure  $\approx 300$  Gbar) and comparable to thermonuclear conditions (thermonuclear ignition in DT occurs at about 4 keV). In 1988, K. Boyer et al. [24] investigated the possibility that such laser beams could be focussed onto solid surfaces and cause nuclear transitions. In particular, irradiation of a uranium target could induce electro- and photo-fission in the focal region.

These developments open the possibility of “switching” nuclear reactions on and off by high intensity ultraviolet laser radiation and providing a bright point source of fission products and neutrons.

### Laser-Induced Radioactivity

When a laser pulse of intensity  $10^{19}$  W cm $^{-2}$  interacts with solid targets, electrons of energies of some tens of MeV are produced. In a tantalum target, the electrons generate an intense highly directional  $\gamma$ -ray beam that can be used to carry out photo-nuclear reactions. The isotopes  $^{11}\text{C}$ ,  $^{38}\text{K}$ ,  $^{62,64}\text{Cu}$ ,  $^{63}\text{Zn}$ ,  $^{106}\text{Ag}$ ,  $^{140}\text{Pr}$ , and  $^{180}\text{Ta}$  have been produced by ( $\gamma$ , n) reactions using the VULCAN laser beam.

### Laser-Induced Photo-Fission of Actinides – Uranium and Thorium

The first demonstrations were made with the giant pulse VULCAN laser in the U. K. using uranium metal and with the high repetition rate laser at the University of Jena with thorium samples. Both experiments were carried out in collaboration with the Institute for Transuranium Elements in Karlsruhe. Actinide photo-fission

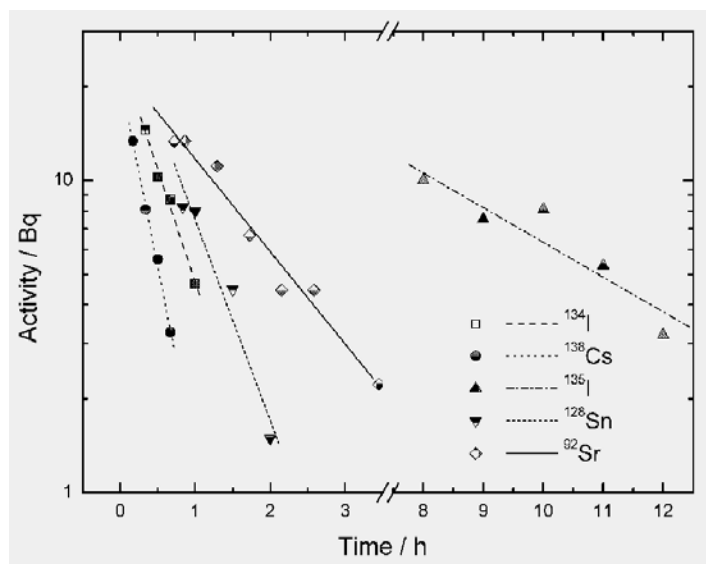


**Fig. 5.6.** Decay characteristics of fission products from bremsstrahlung-induced fission of  $^{232}\text{Th}$ . The deduced half-lives are in good agreement with literature values. Symbols indicate experimental data

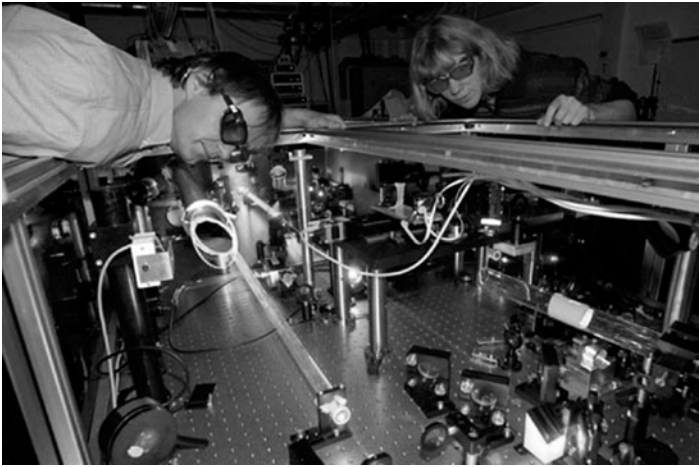


Fig. 5.7. Jena high repetition rate tabletop laser

was achieved in both U and Th using the high-energy bremsstrahlung radiation produced by laser acceleration of electrons. The fission products were identified by time-resolved  $\gamma$ -spectroscopy.

### Laser-Driven Photo-Transmutation of Iodine-129

The first successful laser induced transmutation of  $^{129}\text{I}$ , one of the key radionuclides in the nuclear fuel cycle was reported recently [25–27].  $^{129}\text{I}$  with a half-life of 15.7

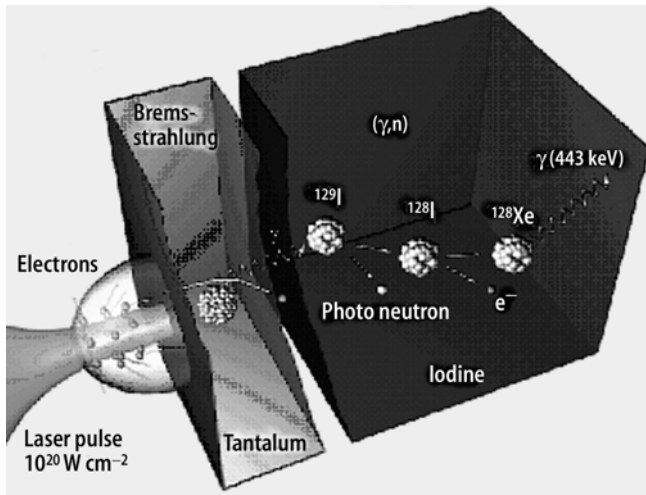
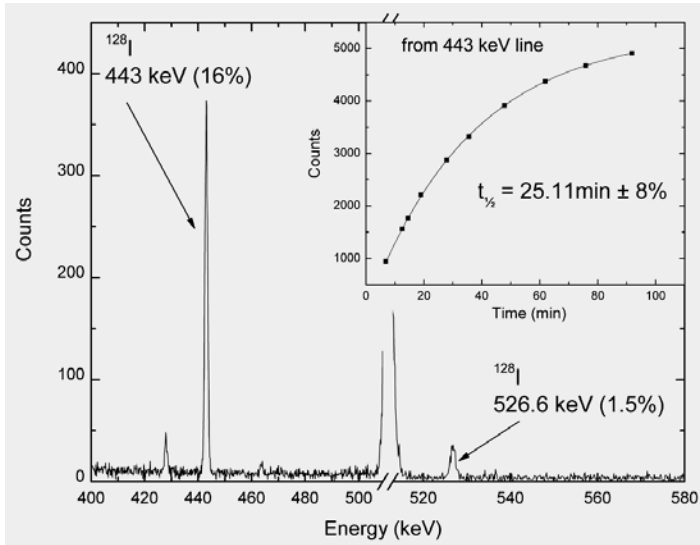


Fig. 5.8. The high intensity laser pulse produces a hot plasma on the surface of a tantalum foil. Relativistic electrons are stopped in the foil, efficiently generating high-energy Bremsstrahlung. The  $^{129}\text{I}$  in the radioactive target is transformed into  $^{128}\text{I}$  due to a  $(\gamma, n)$ -reaction





**Fig. 5.9.** Gamma emission spectra from one of the iodine samples measured before and after laser irradiation of the gold target. Characteristic emission lines of  $^{128}\text{I}$  at 443.3 keV and 527.1 keV are clearly observed, alongside peaks from the decay of  $^{125}\text{Sb}$  impurity and a peak at 511 keV from positron annihilation

million years is transmuted into  $^{128}\text{I}$ , with a half-life of 25 min through a  $(\gamma,n)$ -reaction using laser generated Bremsstrahlung.

### Laser-Induced Heavy Ion Fusion

In a recent series of experiments with the VULCAN laser, at intensities of  $10^{19} \text{ W cm}^{-2}$ , beams of energetic ions were produced by firing the laser onto a thin foil primary target (Fig. 5.10).

The resulting ion beam then interacts with a secondary target. If the ions have enough kinetic energy, it is possible to produce fusion of the ions in the beam with

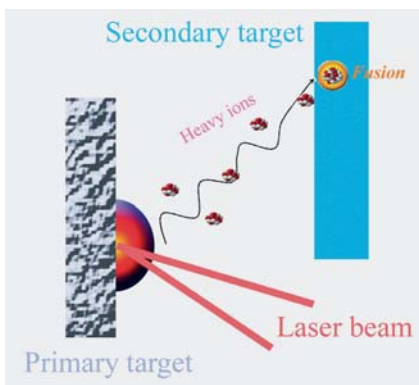


**Fig. 5.10.** Setup of the heavy ion fusion experiment. The laser is focussed onto a primary target (Al, C or other), where it generates a hot plasma on the surface. Heavy ions accelerated in the plasma are blown-off into the secondary target (Al, Ti, Zn, or other) inducing a fusion reaction

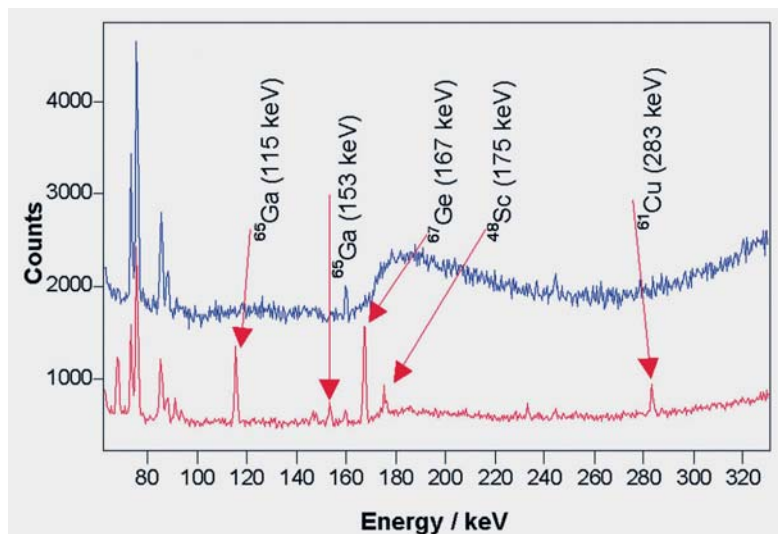


**Fig. 5.11.** The main reaction products identified by their characteristic gamma emission for a Ti plate exposed to Al blow-off. Blue spectrum: “cold” target, red spectrum, heated target (391 °C). Fusion products are much more evident in the heated target

atoms in the secondary target. Heavy ion beams were generated from primary targets of aluminium and carbon. Secondary target material consisted of aluminium, titanium, iron and zinc niobium and silver. The heavy ion “blow-off” fused with the atoms in the secondary target creating compound nuclei in highly excited states. The compound nuclei then de-excited to create fusion products in the secondary target foils. These foils were then examined in a high efficiency germanium detector to

**Table 5.1.** Heavy ions fusion measurement. The primary and secondary target materials are given, with some of the measured and identified fusion products

Primary target material	Secondary target	Nuclides identified in preliminary analysis
Al	Al	$^{49}\text{Cr}$ , $^{27}\text{Mg}$ , $^{28}\text{Al}$ , $^{43}\text{Sc}$ , $^{34\text{m}}\text{Cl}$
Al (heated)	Ti	$^{48}\text{V}$ , $^{44}\text{Sc}$ , $^{48}\text{Sc}$ , $^{65}\text{Ga}$ , $^{67}\text{Ge}$ , $^{61}\text{Cu}$ , $^{70}\text{As}$
C	Fe	$^{65,66}\text{Ga}$ , $^{67}\text{Ge}$ , $^{60}\text{Cu}$ , $^{63}\text{Zn}$
C	Ag	$^{117}\text{Te}$ , $^{115}\text{Te}$ , $^{119}\text{I}$

measure the characteristic gamma radiation produced by the radioactive decay of short-lived fusion product nuclides. Typical spectra are shown in Fig. 5.11.

Figure 5.11 shows the results of experiments involving cold and heated targets. The target here was aluminium, and the secondary titanium. The spectrum in blue is that taken for the aluminium target at room temperature, and the red spectrum is that of an aluminium target heated to 391 °C. For the heated target, many more fusion products are evident which are not observed in the cold target. This is attributed to the heating of the target to remove hydrocarbon impurities. When these layers are removed, heavier ions are accelerated more readily and to higher energies.

### Laser-Driven (p,xn)-Reactions on Lead

Recently, (p,xn) reactions on lead with the use of very high intensity laser radiation has been demonstrated. Laser radiation is focused onto a thin foil to an intensity of  $10^{20} \text{ W cm}^{-2}$  to produce a beam of high-energy protons. These protons interact with a lead target to produce (p,xn) reactions. The (p,xn) process is clearly visible through the production of a variety of bismuth isotopes with natural lead. Such experiments may provide useful basic nuclear data for transmutation in the energy range 20–250 MeV without recourse to large accelerator facilities.

Spallation nuclear reactions refer to non-elastic interactions induced by a high-energy particle in which mainly neutrons are “spalled,” or knocked out of the nucleus directly, followed by the evaporation of low energy particles as the excited nucleus heats up. At low energies ( $\leq 50 \text{ MeV}$ ), the de Broglie wavelength of the proton is larger than the size of individual nucleons. The proton then interacts with the entire nucleus and a compound nucleus is formed. At high proton energies ( $\geq 50 \text{ MeV}$ ), the de Broglie wavelength is of the order of the nucleon dimensions. The proton can interact with single or a few nucleons and results in direct reactions. These latter reactions are referred to as spallation nuclear reactions and refer to non-elastic interactions induced by a high-energy particle in which mainly light charged particles and neutrons are “spalled,” or knocked out of the nucleus directly, followed by the evaporation of low energy particles as the excited nucleus heats up. Current measurements on the feasibility of proton induced spallation of lead and similar materials focus around the need to measure nuclear reaction cross-sections relevant to accelerator driven systems desirable for use in the transmutation of long-lived radioactive products in nuclear waste. The neutron production from the spallation reaction is important for defining the proton beam energy and target requirements. However the measurements being undertaken require high power accelerators to generate the proton beam. In the present work, the proton beam is generated by a high-intensity laser rather than by an accelerator.

The recently developed petawatt arm of the VULCAN Nd:glass laser at the Rutherford Appleton Laboratory, UK, was used in this experiment. The 60 cm beam was focused to a  $7.0 \mu\text{m}$  diameter spot using a 1.8 m focal length off-axis parabolic mirror, in a vacuum chamber evacuated to  $\sim 10^{-4}$  mbar (Fig. 5.12). P-polarised laser pulses with energy up to 400 J, wavelength  $\sim 1 \mu\text{m}$  and average duration 0.7 ps, were focused onto foil targets at an angle of  $45^\circ$  and to an intensity of the order of

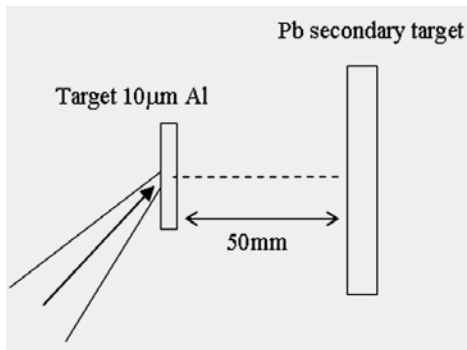


**Fig. 5.12.** Experimental setup for the laser production of protons and ions. The protons or Al ions generated from the laser irradiation of the target foil are used for nuclear activation in the secondary target

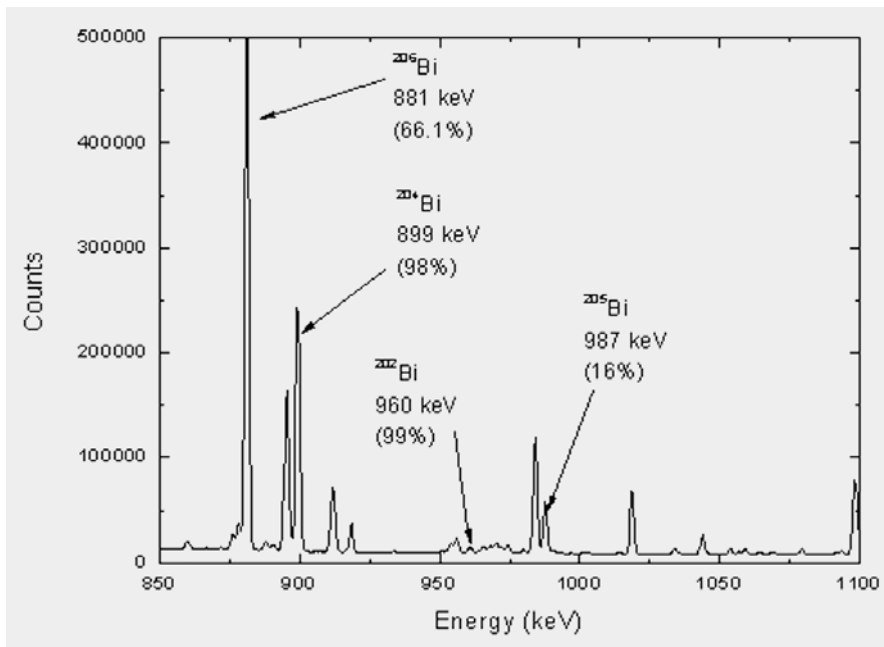


**Fig. 5.13.** Preliminary identification of bismuth isotopes produced through (p,xn) reactions in lead

$4 \times 10^{20} \text{ W cm}^{-2}$ . A typical spectrum resulting from the proton activation of lead to produce bismuth isotopes is shown in Fig. 5.13 (the relevant section of the nuclide chart is shown in Fig. 5.14).

The protons originate from  $\text{H}_2\text{O}$  and hydrocarbon contamination layers on the surface of solid targets. Secondary catcher activation samples were positioned at the front of the target (the ‘blow-off’ direction). Energetic protons accelerated from the primary target foil can induce nuclear reactions in these activation samples.

From the proton induced reactions on lead, the isotopes  $^{202}\text{--}^{206}\text{Bi}$  were identified using the main emission lines.

Po203 36,7 m	Po204 3,53 h	Po205 1,66 h	Po206 8,8 d	Po207 5,8 h	Po208 2,9 y	Po209 1,0E2 y	Po210 1,4E2 d
Bi202 1,72 h	Bi203 11,76 h	Bi204 11,22 h	Bi205 15,31 d	Bi206 6,24 d	Bi207 31,57 y	Bi208 3,7E5 y	Bi209 stable 100%
Pb201 9,33 h	Pb202 5,3E4 y	Pb203 2,16 d	Pb204 stable 1,4%	Pb205 1,5E7 y	Pb206 stable 24,1%	Pb207 stable 22,1%	Pb208 stable 52,4%
Tl200 1,09 d	Tl201 3,04 d	Tl202 12,23 d	Tl203 stable 29,524%	Tl204 3,78 y	Tl205 stable 70,476%	Tl206 4,2 m	Tl207 4,77 m
Hg199 stable 16,07%	Hg200 stable 23,1%	Hg201 stable 13,16%	Hg202 stable 29,86%	Hg203 46,61 d	Hg204 stable 6,87%	Hg205 5,2 m	Hg206 8,15 m

Fig. 5.14. Nuclide chart [31] showing the location of lead and bismuth isotopes

### Laser Activation of Micro-Spheres

Nano-encapsulation of chemical agents is well known in the pharmaceutical field. Nano-radiotherapy is a technique in which nano-particles can be made radioactive and then used in cancer therapy [28–29]. Nano-spheres are relatively easy to manufacture and the isotope to be activated is chosen depending on the type and size of the tumour. The particles are activated by neutron irradiation in a nuclear reactor. Typically, durable ceramic micro-spheres containing a large amount of yttrium and/or phosphorus are useful for *in situ* radiotherapy of cancer, since the stable  $^{89}\text{Y}$

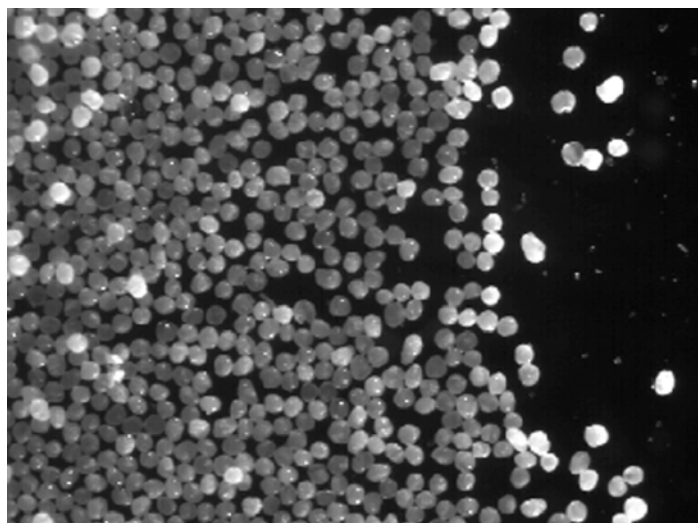


Fig. 5.15. Zirconium oxide micro-particles. The particle diameters are in the range 95–110  $\mu\text{m}$

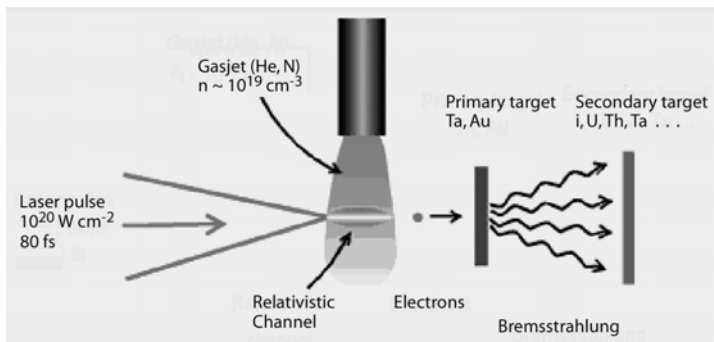


Fig. 5.16. Setup for the laser micro-particle irradiation experiments

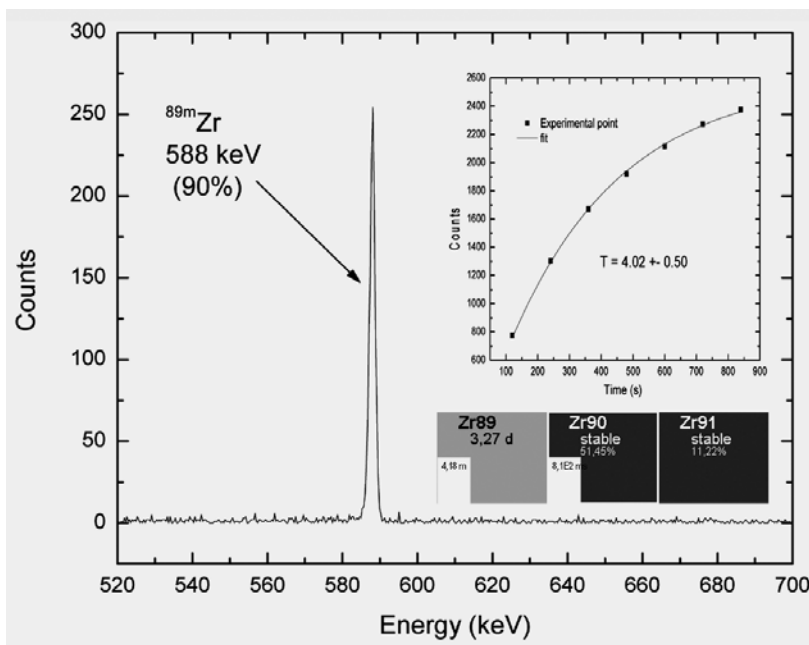
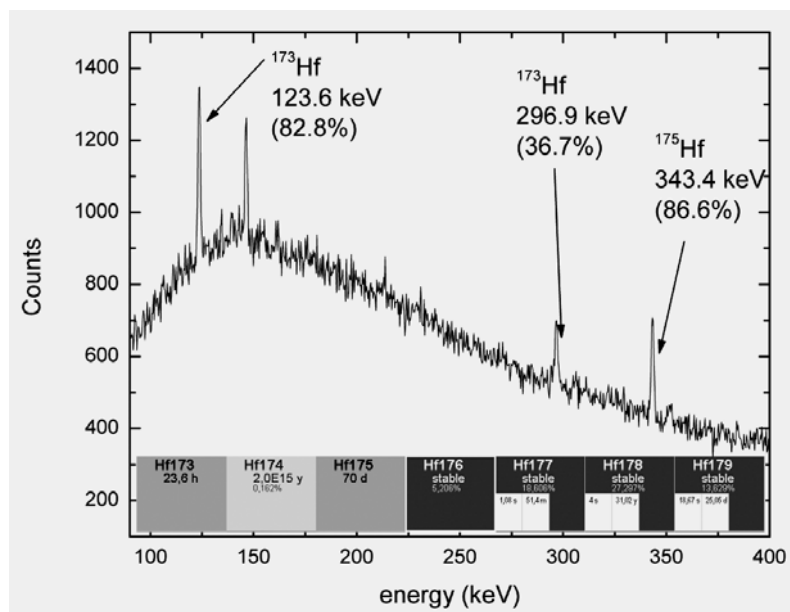


Fig. 5.17. Spectra taken 10 min. after the Zr irradiation showing the main line of <sup>89m</sup>Zr from the <sup>90</sup>Zr( $\gamma, n$ )<sup>89m</sup>Zr reaction. The inset shows the position of the isotopes in the nuclide chart (from Nuclides.net [31])

and/or <sup>31</sup>P in the micro-spheres can be activated to  $\beta$ -emitters <sup>90</sup>Y with a half-life: 2.7 d and/or <sup>32</sup>P with a half-life of 14.3 d.

Recently, micro-particles have been activated in a ultra high intensity laser field for the first time [30]. Micro-particles of ZrO<sub>2</sub> and HfO<sub>2</sub>, with diameters of approximately 80  $\mu$ m, were irradiated using the high repetition rate laser at the University of Jena (see Fig. 5.15).



**Fig. 5.18.** Spectrum showing the lines of the  $^{173}\text{Hf}$  and  $^{175}\text{Hf}$  from the laser irradiation of the  $\text{HfO}_2$ . The inset shows the position of the hafnium isotopes in the nuclide chart (from Nuclides.net [31])

Focussing the laser beam in the gas jet (Fig. 5.16) results in a high temperature plasma. Relativistic self-focussing of the electrons gives rise to a directed, pulsed, high-energetic electron beam which interacts with the primary target to produce high-energy bremsstrahlung. This bremsstrahlung is then used for the particle activation. The results are shown for both the zirconium and hafnium micro-particles in Figs. 5.17 and 5.18.

The future development of the field of laser transmutation will benefit from the currently fast evolution of high intensity laser technology. Within a few years, compact and efficient laser systems will emerge, capable of producing intensities exceeding  $10^{22} \text{ W cm}^{-2}$  with repetition rates of 1 shot per minute and higher. These laser pulses will generate electron and photon temperatures in the range of the giant dipole resonances and open the possibility of obtaining nuclear data in this region. These laser experiments may offer a new approach to studying material behaviour under neutral and charged particle irradiation without resource to nuclear reactors or particle accelerators.